Direct Power Control of a Pulse Width Modulation Rectifier Using Space Vector Modulation Under Unbalanced Grid Voltages

Yongchang Zhang, *Member, IEEE*, and Changqi Qu, *Student Member, IEEE*

***Abstract*—Compared with conventional table-based direct power control (DPC), DPC using space vector modulation (DPC-SVM) exhibits several specific features, such as a constant switching frequency and small ripples in both active power and reactive power. However, conventional DPC-SVM exhibits highly distorted grid currents when the grid voltages are unbalanced. In this study, we propose a novel and simple DPC-SVM that is effective under both ideal and unbalanced grid voltage conditions by using an extension of original instantaneous power theory. After deducing the power slopes of both active power and reactive power, the suitable converter voltage reference to nullify the errors of active power and reactive power is analytically derived, which is subsequently synthesized by SVM. The proposed DPC-SVM does not require the extraction of complex positive/negative sequence from the grid voltage/current or power compensation. Compared to prior DPC-SVM using original imaginary power, the proposed method exhibits much better performance by obtaining highly sinusoidal line currents and eliminating twice grid-frequency ripples in both active power and the reactive power under unbalanced conditions. Simulations and experimental results supported the theoretical study and confirmed the effectiveness of the proposed method.**

***Index Terms*—Direct power control (DPC), pulse width modulation (PWM) rectifier, reactive power control, space vector modulation (SVM).**

I. Introduction

PULSE width modulation (PWM) rectifiers have attracted widespread attention because of their advantages in terms of bidirectional power flow, sinusoidal line current, controllable input power factor, good dc-link voltage regulation ability [1], [2], and other features. Currently, the most popular high-performance control methods for PWM rectifiers are voltage-oriented control (VOC) [3] and direct power control (DPC) [4]–[6]. VOC decomposes the grid currents into active power component and reactive power component in synchronous frame, which are regulated by inner current loops using PI controllers. The obtained converter voltage vector references are subsequently synthesized by space vector modulation (SVM). Good steady-state performance and quick response can be obtained in VOC, but it requires fine tuning work and accurate system parameters.

DPC has many obvious advantages, such as its simple structure and rapid dynamic response; thus, this method is attracting increasing attention [4]–[9]. Compared to VOC, neither internal current-control loops nor PWM modulator block are required in table-based DPC. It selects the desired voltage vector directly for active and reactive power regulation based on a predefined switching table and grid voltage position [4], [9]. However, table-based DPC produces large power ripples and the switching frequency is variable, which is mainly caused by the use of heuristic switching table and hysteresis comparators. To improve the steady-state performance, predictive control methods have been introduced to replace the switching table to achieve more accurate and effective vector selection [10]–[13]. However, they are relatively complicated and relies on the accuracy of system parameters.

Recently, a control strategy called DPC-SVM was proposed [5], [14], [15], which combines the advantages of both table-based DPC and VOC. Compared with table-based DPC, DPC-SVM presents several advantages, such as small ripples in active and reactive power, a constant switching frequency, and a lower current harmonic [5]. The PI controllers in power loops [5] can be further eliminated if predictive deadbeat power control is used, as shown in [14].

So far, the control strategies for DPC have been studied in depth under ideal grid voltage conditions. However, in actual conditions the grid voltages are usually unbalanced, which may be caused by single-phase load, grid impedance unbalances, voltage dip, and so on [16]. Thus, a PWM rectifier designed for ideal grid conditions may exhibit an abnormal operating state, such as harmonics in the dc output and odd harmonics in the input currents [17], [18]. Some studies have attempted to mitigate the influence of unbalance grid voltages on DPC. For example, in [19] a power compensation block is added to the reference value of active power and reactive power to achieve sinusoidal and balanced grid currents. However, oscillations can be found in both active power and reactive power. Furthermore, it requires the decomposition of positive and negative sequences of both grid voltage and currents. The power compensation block was simplified in [20] by eliminating the extraction of the negative sequence current. Unfortunately, it is still necessary to extract the negative sequence grid voltages and positive sequence grid

Manuscript received July 10, 2014; revised October 2, 2014; accepted November 13, 2014. Date of publication November 20, 2014; date of current version May 22, 2015. This work was supported by the National Natural Science Foundation of China under Grant 51207003 and Grant 51347004, Beijing Nova Program under Grant xx2013001, Chongqing Natural Science Foundation under Grant cstc2012jjB107, and Open Research Fund from Key Laboratory of Special Power Supply under Grants MSPS2012-03 and MSPS2013-02. Recommended for publication by Associate Editor A. M. Trzynadlowski.

The authors are with Power Electronics and Motor Drives Engineering Research Center, North China University of Technology, Beijing 100144, China, and also with Collaborative Innovation Center of Electric Vehicles in Beijing. (e-mail: yozhang@ieee.org; qcqdhr@sina.com).

Color versions of one or more of the figures in this paper are available online at http://ieeexplore.ieee.org.

Digital Object Identifier 10.1109/TPEL.2014.2371469

currents to achieve appropriate power compensation. Hence, it is desirable to eliminate the sequence extraction of grid voltage and currents for DPC under unbalanced grid voltage conditions.

Most study regarding PWM rectifier adopts the instantaneous power theory (also called pq theory) proposed by Akagi *et al.*[21]. However, it has been shown that the instantaneous imaginary power in the original pq theory is unsuitable for unbalanced input supply, as shown in [18], [22], and [23], and confirmed in this paper. It has been widely accepted that the instantaneous reactive power can be expressed by the voltages lagging the actual voltage by 90°, especially under unblanced grid voltage conditions. This extended pq theory was firstly proposed in 1995 by Komastu and Kawabata [22] in abc frame and later expressed using complex vectors in *dq*-frame in 2006 by Suh and Lipo [18]. In spite of the merits of the extended pq theory, it was mainly studied in the frame of VOC [18], [24], requiring complicated current reference calculations and extraction of the positive and negative sequences of grid voltage/currents. To reduce the control complexity in [18] and [24], the current reference was calculated in stationary frame using grid voltages and converter voltages, as well as their respective delayed value [25] and, then, proportional plus resonant (PR) controller is employed to track the current reference. Although sinusoidal line current and small ripple in dc voltage were obtained, the method in [25] uses the grid current as control variable and its performance depends largely on the tuning work of PR. Furthermore, it did not evaluate the performance of controller if original imaginary power [21] is used in the control method.

So far, the extended pq theory, [18], [22], [23], has not been fully investigated in the frame of DPC. This paper fills this gap by proposing a novel and simple DPC-SVM method, which adopts the extended pq theory to analytically derive the desired converter voltage reference for nullifying the errors of active power and reactive power, especially under unbalanced conditions. Compared to the prior DPC-based solutions using original imaginary power [19], [20], the proposed DPC-SVM does not require power compensation and the extraction of complicated positive/negative sequences from the grid voltage/current. Compared to the SVM-based solution using the extended pq theory [18], [25], the proposed DPC-SVM is a true power control method rather than current control. Furthermore, it does not require any tuning work in the controller, which is quick to use and simple to implement by reducing the tuning effort and control complexity. In fact, the proposed DPC-SVM uses almost the same control structure as conventional DPC-SVM [14], except that the original imaginary power is replaced by the reactive power in the extended pq theory. So, it is possible to improve the performance of conventional DPC-SVM under unbalanced grid voltage conditions with low effort. Of course, all the relevant formulas have to be deduced again to be in accordance with the extended pq theory, as shown in this paper. The merits of quick response, fixed switching frequency and low tuning work in conventional DPC-SVM are fully reserved in the proposed method. The practical issue of control delay compensation is also considered when calculating the voltage vector reference, which was not explicitly considered in prior DPC-SVM methods [5], [14]. The effectiveness of the proposed method is validated by both simulation and experimental results.

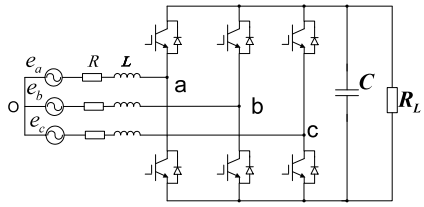

Fig. 1. Topology of a two-level PWM rectifier.

II. PWM Rectifier Model

The circuit of a three-phase PWM rectifier is shown in Fig. 1, and its mathematical model can be expressed in stationary two-phase coordinate as [6], [12]

$$\boldsymbol{e} = R\boldsymbol{i} + L\frac{d\boldsymbol{i}}{dt} + \boldsymbol{v} \tag{1}$$

where $\boldsymbol{v}$, $\boldsymbol{e}$, and $\boldsymbol{i}$ are the converter voltage vector, the grid voltage vector and the grid current vector, respectively, R and L are the equivalent series resistance and inductance of grid filter.

According to the original pq theory introduced in [21], the complex power $\boldsymbol{s}$ in the grid side can be expressed as

$$\boldsymbol{s} = \frac{3}{2}\left(\boldsymbol{i}^*\boldsymbol{e}\right) \tag{2}$$

where $*$ denotes the conjugate of a complex vector.

The instantaneous active power (or real power) p and imaginary power q can be expressed as

$$p = \ \mathrm{Re}(\boldsymbol{S}) = \frac{3}{2}\mathrm{Re}\left(\boldsymbol{i}^*\boldsymbol{e}\right) \tag{3}$$

$$q = \ \mathrm{Im}(\boldsymbol{S}) = \frac{3}{2}\mathrm{Im}\left(\boldsymbol{i}^*\boldsymbol{e}\right). \tag{4}$$

As the original pq theory is unsuitable to work under unbalanced grid voltage conditions, in this study, we use the extended pq theory proposed in [18], [22], and [23], where the instantaneous reactive power is expressed as

$$q^{\mathrm{nov}} = \frac{3}{2}\mathrm{Re}\left(\boldsymbol{i}^*\boldsymbol{e}^{'}\right) \tag{5}$$

The variable $\boldsymbol{e}^{'}$ lags $\boldsymbol{e}$ by 90 electrical degrees [18], [22], [23], which is corresponding to a quarter of fundamental period [26].

Under unbalanced grid conditions, the grid voltage and grid current can be expressed as the sum of positive sequence and negative sequence components [16], [18], [27]

$$\boldsymbol{e} = \ \boldsymbol{e}^+ + \boldsymbol{e}^- = \boldsymbol{e}^+_{dq}e^{j\omega t} + \boldsymbol{e}^-_{dq}e^{-j\omega t} \tag{6}$$

$$\boldsymbol{i} = \ \boldsymbol{i}^+ + \boldsymbol{i}^- = \boldsymbol{i}^+_{dq}e^{j\omega t} + \boldsymbol{i}^-_{dq}e^{-j\omega t} \tag{7}$$

and the delayed value of unbalanced grid voltages $\boldsymbol{e}^{'}$ can be expressed as

$$\begin{aligned}\boldsymbol{e}^{'} &= \ \boldsymbol{e}^+_{dq}e^{j(\omega t-\frac{\pi}{2})} + \boldsymbol{e}^-_{dq}e^{-j(\omega t-\frac{\pi}{2})} \\ &= \ -j\boldsymbol{e}^+_{dq}e^{j\omega t} + j\boldsymbol{e}^-_{dq}e^{-j\omega t} = -j\boldsymbol{e}^+ + j\boldsymbol{e}^-\end{aligned} \tag{8}$$

where $\boldsymbol{e}_{dq}^{+} = e_d^{+} + \mathrm{j}e_q^{+}$, $\boldsymbol{i}_{dq}^{+} = i_d^{+} + \mathrm{j}i_q^{+}$ denotes the positive sequence component of the grid voltage/current in the positive synchronous frame; $\boldsymbol{e}_{dq}^{-} = e_d^{-} + \mathrm{j}e_q^{-}$, $\boldsymbol{i}_{dq}^{-} = i_d^{-} + \mathrm{j}i_q^{-}$ represents the negative sequence component of the grid voltage/current in the negative synchronous frame. In this study, it is assumed that the grid frequency is $\omega = 2\pi \times 50 = 314$ rad/s.

Under unbalanced grid conditions, the active power and reactive power can be expressed as

$$\begin{aligned} p &= \frac{3}{2}\mathrm{Re}\left(\boldsymbol{i}^{*}\boldsymbol{e}\right) \\ &= \frac{3}{2}\mathrm{Re}\left[\left(\boldsymbol{i}_{dq}^{+}e^{j\omega t} + \boldsymbol{i}_{dq}^{-}e^{-j\omega t}\right)^{*} \cdot \left(\boldsymbol{e}_{dq}^{+}e^{j\omega t} + \boldsymbol{e}_{dq}^{-}e^{-j\omega t}\right)\right] \end{aligned} \tag{9}$$

$$\begin{aligned} q^{\mathrm{nov}} &= \frac{3}{2}\mathrm{Re}\left(\boldsymbol{i}^{*}\boldsymbol{e}^{'}\right) = \frac{3}{2}\mathrm{Re}\left[\boldsymbol{i}^{*}\boldsymbol{e}\left(t - \frac{T}{4}\right)\right] \\ &= \frac{3}{2}\mathrm{Re}\Bigg[\left(\boldsymbol{i}_{dq}^{+}e^{j\omega t} + \boldsymbol{i}_{dq}^{-}e^{-j\omega t}\right)^{*} \\ &\quad \cdot \left(-j \cdot \boldsymbol{e}_{dq}^{+}e^{j\omega t} + j \cdot \boldsymbol{e}_{dq}^{-}e^{-j\omega t}\right)\Bigg] \end{aligned} \tag{10}$$

where T is the fundamental period of grid voltages.

Expanding (9) and (10), they can be further arranged in the following form as:

$$p = P_0 + P_{c2}\cos\left(2\omega t\right) + P_{s2}\sin\left(2\omega t\right) \tag{11}$$

$$q^{\mathrm{nov}} = Q_0 + Q_{c2}\cos\left(2\omega t\right) + Q_{s2}\sin\left(2\omega t\right) \tag{12}$$

where

$$P_0 = \frac{3}{2}\left(\boldsymbol{i}_{dq}^{+} \odot \boldsymbol{e}_{dq}^{+} + \boldsymbol{i}_{dq}^{-} \odot \boldsymbol{e}_{dq}^{-}\right) \tag{13}$$

$$P_{c2} = \frac{3}{2}\left(\boldsymbol{i}_{dq}^{+} \odot \boldsymbol{e}_{dq}^{-} + \boldsymbol{i}_{dq}^{-} \odot \boldsymbol{e}_{dq}^{+}\right) \tag{14}$$

$$P_{s2} = \frac{3}{2}\left(\boldsymbol{i}_{dq}^{+} \otimes \boldsymbol{e}_{dq}^{-} - \boldsymbol{i}_{dq}^{-} \otimes \boldsymbol{e}_{dq}^{+}\right) \tag{15}$$

and

$$Q_0 = \frac{3}{2}\left(\boldsymbol{i}_{dq}^{+} \otimes \boldsymbol{e}_{dq}^{+} - \boldsymbol{i}_{dq}^{-} \otimes \boldsymbol{e}_{dq}^{-}\right) \tag{16}$$

$$Q_{c2} = \frac{3}{2}\left(-\boldsymbol{i}_{dq}^{+} \otimes \boldsymbol{e}_{dq}^{-} + \boldsymbol{i}_{dq}^{-} \otimes \boldsymbol{e}_{dq}^{+}\right) \tag{17}$$

$$Q_{s2} = \frac{3}{2}\left(\boldsymbol{i}_{dq}^{+} \odot \boldsymbol{e}_{dq}^{-} + \boldsymbol{i}_{dq}^{-} \odot \boldsymbol{e}_{dq}^{+}\right) \tag{18}$$

From (14), (15), (17), and (18) it is clearly seen that $P_{c2} = Q_{s2}$, $P_{s2} = -Q_{c2}$. This means that the ripple amplitude of the reactive power is the same as that of active power. In other words, eliminating the oscillation in the reactive power would lead to autonomous ripple cancellation in the active power. This fact is useful because it provides some benefits for control by improving the performance of conventional DPC-SVM under unbalanced grid voltage conditions.

III. Conventional DPC-SVM

Under the assumption of sinusoidal and balanced three-phase grid voltage, i.e., $\boldsymbol{e} = |\boldsymbol{e}|e^{j\omega t}$, the derivative of complex power can be obtained from (1) and (2) as follows [6]:

$$\frac{d\boldsymbol{s}}{dt} = \frac{1}{L}\left[\frac{3}{2}\left(|\boldsymbol{e}|^2 - \boldsymbol{v}^{*}\boldsymbol{e}\right) - (R - j\omega L)\cdot\boldsymbol{s}\right]. \tag{19}$$

In conventional DPC-SVM [14], the control aim is to achieve deadbeat control of complex power. In other words, the complex power should reach its reference value at the end of the next control period, namely $\boldsymbol{s}^{k+1} = \boldsymbol{s}^{\mathrm{ref}}$. According to this principle, the equation in (19) can be discretized using first-order Euler method as

$$\begin{aligned} \frac{\boldsymbol{s}^{\mathrm{ref}} - \boldsymbol{s}^{k}}{T_s} = \frac{1}{L}\Bigg[&\frac{3}{2}\left(\left|\boldsymbol{e}^{k}\right|^2 - \mathrm{conj}\left(\boldsymbol{v}^{k}\right)\cdot\boldsymbol{e}^{k}\right) \\ &- (R - j\omega L)\cdot\boldsymbol{s}^{k}\Bigg] \end{aligned} \tag{20}$$

where T_s is the control period.

Solving (20), the desired converter voltage vector in stationary frame is obtained as

$$\boldsymbol{v}^{k} = \boldsymbol{e}^{k} - (R + j\omega L)\,\boldsymbol{i}^{k} - \frac{2L}{3T_s}\left(\frac{\boldsymbol{s}^{\mathrm{ref}} - \boldsymbol{s}^{k}}{\boldsymbol{e}^{k}}\right)^{*}. \tag{21}$$

The (21) can be expressed in terms of its components as

$$\begin{aligned} \begin{bmatrix} v_\alpha^k \\ v_\beta^k \end{bmatrix} = &\begin{bmatrix} e_\alpha^k \\ e_\beta^k \end{bmatrix} - \begin{bmatrix} R & -\omega L \\ \omega L & R \end{bmatrix}\begin{bmatrix} i_\alpha^k \\ i_\beta^k \end{bmatrix} \\ &- \frac{2L}{3T_s\left|\boldsymbol{e}^{k}\right|^2}\begin{bmatrix} e_\alpha^k & e_\beta^k \\ e_\beta^k & -e_\alpha^k \end{bmatrix}\begin{bmatrix} p^{\mathrm{ref}} - p^k \\ q^{\mathrm{ref}} - q^k \end{bmatrix}. \end{aligned} \tag{22}$$

It should be noted that the second term on the right side of (22) is omitted in [14], because it assumed that $\boldsymbol{e}^{k+1} = \boldsymbol{e}^{k}$. As a result, there is a small offset in the imaginary power, as shown in [14]. On the contrary, the derived converter voltage reference in (22) is complete in theory without any omission, so it should achieve better steady-state performance.

IV. Proposed DPC-SVM

A. Analysis of Reactive Power

The conventional DPC-SVM using (22) was able to achieve fast and accurate tracking of both active power and imaginary power, as shown in [14]. However, the grid current would be highly distorted under unbalanced grid voltages, if the grid unbalanced is not taken into account. It is necessary to investigate the performance of DPC-SVM under unbalanced grid voltages and give appropriate solution, which is one of the motivations of this paper.

In this paper, the control aim of the proposed DPC-SVM is to obtain sinusoidal grid current, while eliminating the oscillations in the active power. To achieve this aim, the reactive power in (5) is used as a control variable in combination with the conventional active power in (3). As analyzed in Section II, oscillation elimination can be simultaneously achieved in both active power and the reactive power. Hence, the specific control aim of the proposed DPC-SVM can be expressed in the

following equations:

$$\begin{cases} P_0 &= \frac{3}{2}\left(\boldsymbol{i}_{dq}^{+}\odot\boldsymbol{e}_{dq}^{+}+\boldsymbol{i}_{dq}^{-}\odot\boldsymbol{e}_{dq}^{-}\right)=p^{\mathrm{ref}} \\ Q_0^{\mathrm{nov}} &= \frac{3}{2}\left(\boldsymbol{i}_{dq}^{+}\otimes\boldsymbol{e}_{dq}^{+}-\boldsymbol{i}_{dq}^{-}\otimes\boldsymbol{e}_{dq}^{-}\right)=0 \\ P_{c2} &= \frac{3}{2}\left(\boldsymbol{i}_{dq}^{-}\odot\boldsymbol{e}_{dq}^{+}+\boldsymbol{i}_{dq}^{+}\odot\boldsymbol{e}_{dq}^{-}\right)=0 \\ P_{s2} &= \frac{3}{2}\left(\boldsymbol{i}_{dq}^{+}\otimes\boldsymbol{e}_{dq}^{-}-\boldsymbol{i}_{dq}^{-}\otimes\boldsymbol{e}_{dq}^{+}\right)=0. \end{cases} \tag{23}$$

Solving (23), the desired current reference in terms of positive sequence and negative sequence current can be obtained [27]. However, it results in complicated expression and involves the positive sequence and negative sequence extraction of grid voltage, which is also complicated.

In this paper, the sequence extraction of grid voltages and currents are to be avoided. Considering that the calculation of the reactive power requires the delayed value of grid voltage, and to simplify the analysis, a set of variables that lag the voltages and currents by 90 electrical degrees in time domain will be used in the following discussions, where $\boldsymbol{x}^{'}$ denotes the variable that lags $\boldsymbol{x}$ by 90 electrical degrees [25]. According to (6) and (8), the relationship between $\boldsymbol{x}$, $\boldsymbol{x}^{'}$ and $\boldsymbol{x}_{dq}^{+}$, $\boldsymbol{x}_{dq}^{-}$ can be obtained as

$$\begin{bmatrix}\boldsymbol{x}\\ \boldsymbol{x}^{'}\end{bmatrix}=\begin{bmatrix}e^{j\omega t} & e^{-j\omega t}\\ -je^{j\omega t} & je^{-j\omega t}\end{bmatrix}\begin{bmatrix}\boldsymbol{x}_{dq}^{+}\\ \boldsymbol{x}_{dq}^{-}\end{bmatrix}. \tag{24}$$

Solving (24), the positive sequence and negative sequence vector are obtained as

$$\begin{bmatrix}\boldsymbol{x}_{dq}^{+}\\ \boldsymbol{x}_{dq}^{-}\end{bmatrix}=\frac{1}{2}\begin{bmatrix}e^{-j\omega t} & je^{-j\omega t}\\ e^{j\omega t} & -je^{j\omega t}\end{bmatrix}\begin{bmatrix}\boldsymbol{x}\\ \boldsymbol{x}^{'}\end{bmatrix} \tag{25}$$

Substituting (25) into (13) to (18), the gains are now expressed by the variables and their delayed value in stationary frame as

$$P_0 = \frac{3}{4}\left(\boldsymbol{i}\odot\boldsymbol{e}+\boldsymbol{i}^{'}\odot\boldsymbol{e}^{'}\right) \tag{26}$$

$$P_{c2} = \frac{3}{4}\left(k_1\cos(2\omega t)+k_2\sin(2\omega t)\right) \tag{27}$$

$$P_{s2} = \frac{3}{4}\left(-k_2\cos(2\omega t)+k_1\sin(2\omega t)\right) \tag{28}$$

and

$$Q_0 = \frac{3}{4}\left(\boldsymbol{i}\odot\boldsymbol{e}^{'}-\boldsymbol{i}^{'}\odot\boldsymbol{e}\right) \tag{29}$$

$$Q_{c2} = \frac{3}{4}\left(k_2\cos(2\omega t)-k_1\sin(2\omega t)\right) \tag{30}$$

$$Q_{s2} = \frac{3}{4}\left(k_1\cos(2\omega t)+k_2\sin(2\omega t)\right) \tag{31}$$

where $k_1=\boldsymbol{i}\odot\boldsymbol{e}-\boldsymbol{i}^{'}\odot\boldsymbol{e}^{'}$ and $k_2=\boldsymbol{i}\odot\boldsymbol{e}^{'}+\boldsymbol{i}^{'}\odot\boldsymbol{e}$.

From (26) to (31), the equations in (23) are now rewritten as

$$\begin{cases} P_0 &= \frac{3}{4}\left(\boldsymbol{i}\odot\boldsymbol{e}+\boldsymbol{i}^{'}\odot\boldsymbol{e}^{'}\right)=p^{\mathrm{ref}} \\ Q_0^{\mathrm{nov}} &= \frac{3}{4}\left(\boldsymbol{i}\odot\boldsymbol{e}^{'}-\boldsymbol{i}^{'}\odot\boldsymbol{e}\right)=0 \\ P_{c2} &= \frac{3}{4}\left(k_1\cos(2\omega t)+k_2\sin(2\omega t)\right)=0 \\ P_{s2} &= \frac{3}{4}\left(-k_2\cos(2\omega t)+k_1\sin(2\omega t)\right)=0. \end{cases} \tag{32}$$

Solving (32) is equivalent to solving the following equations:

$$\begin{cases} P_0 &= \frac{3}{4}\left(\boldsymbol{i}\odot\boldsymbol{e}+\boldsymbol{i}^{'}\odot\boldsymbol{e}^{'}\right)=p^{\mathrm{ref}} \\ Q_0^{\mathrm{nov}} &= \frac{3}{4}\left(\boldsymbol{i}\odot\boldsymbol{e}^{'}-\boldsymbol{i}^{'}\odot\boldsymbol{e}\right)=0 \\ k_1 &= \boldsymbol{i}\odot\boldsymbol{e}-\boldsymbol{i}^{'}\odot\boldsymbol{e}^{'}=0 \\ k_2 &= \boldsymbol{i}\odot\boldsymbol{e}^{'}+\boldsymbol{i}^{'}\odot\boldsymbol{e}=0. \end{cases} \tag{33}$$

From (33), the final current reference vector is calculated as

$$\boldsymbol{i}^{\mathrm{ref}}=j\frac{-\frac{2}{3}\boldsymbol{e}^{'}}{\boldsymbol{e}\otimes\boldsymbol{e}^{'}}p^{\mathrm{ref}}. \tag{34}$$

It should be noted that the obtained current reference in (34) is equivalent to the current reference in (22) of [25], except that we use complex vector rather than $\alpha\beta$ components in [25], which is more compact and concise in expression. However, it must be pointed that there are notable distinctions between our paper and Li *et al.* [25].

In [25], after obtaining current reference, the PR controller is employed to track the current reference, which still requires some tuning work (although it is simpler than the dual current controller in [18]). The method in [25] still uses the grid current as control variable and requires fine tuning work to achieve good performance.

Contrary to this, the proposed DPC-SVM is a true power control strategy, and it features the merits of simplicity and low tuning work. In fact, from (34), the corresponding new power references satisfying (23) under unbalanced grid voltage conditions can be obtained as

$$\begin{aligned} p_{\mathrm{new}}^{\mathrm{ref}} &= \frac{3}{2}\left(\boldsymbol{i}^{\mathrm{ref}}\odot\boldsymbol{e}\right)=\frac{-p^{\mathrm{ref}}}{\boldsymbol{e}\otimes\boldsymbol{e}^{'}}\left(j\boldsymbol{e}^{'}\odot\boldsymbol{e}\right) \\ &= \frac{-p^{\mathrm{ref}}}{\boldsymbol{e}\otimes\boldsymbol{e}^{'}}\left(\boldsymbol{e}^{'}\otimes\boldsymbol{e}\right)=p^{\mathrm{ref}} \end{aligned} \tag{35}$$

$$\begin{aligned} q_{\mathrm{new}}^{\mathrm{ref}} &= \frac{3}{2}\left(\boldsymbol{i}^{\mathrm{ref}}\odot\boldsymbol{e}^{'}\right)=\frac{-p^{\mathrm{ref}}}{\boldsymbol{e}\otimes\boldsymbol{e}^{'}}\left(j\boldsymbol{e}^{'}\odot\boldsymbol{e}^{'}\right) \\ &= \frac{-p^{\mathrm{ref}}}{\boldsymbol{e}\otimes\boldsymbol{e}^{'}}\left(\boldsymbol{e}^{'}\otimes\boldsymbol{e}^{'}\right)=0. \end{aligned} \tag{36}$$

It is surprising to find that the resulting power references are exactly the same as original power reference using pq theory under balanced grid voltage conditions. This finding indicates that it is possible to achieve performance improvement of conventional DPC-SVM under grid unbalances without modifying the control structure. In fact, it is only necessary to replace the original imaginary power [14] with the reactive power [18], [22] in our method. On the contrary, if imaginary power is used in DPC-SVM, the qualify of grid current would be deteriorated seriously, as shown in the simulation and experimental results. The remaining work is how to track the power reference accurately and quickly, as shown in Section IV-B. Note that the calculation of the current or power reference is based on the assumption that only negative sequence component exist in the grid current, the proposed DPC-SVM not only achieves oscillation elimination in both active power and reactive power, but also produces sinusoidal current without harmonics in theory.

B. Deadbeat Control of Active Power and the Reactive Power

From (6) and (8), the differentiation of grid voltage vector and its delayed value can be obtained as

$$\frac{d\boldsymbol{e}}{dt} = j\omega\boldsymbol{e}^{+} - j\omega\boldsymbol{e}^{-} = -\omega\boldsymbol{e}^{'} \tag{37}$$

$$\frac{d\boldsymbol{e}^{'}}{dt} = \omega\boldsymbol{e}^{+} + \omega\boldsymbol{e}^{-} = \omega\boldsymbol{e}. \tag{38}$$

The differentiation of grid current can be obtained from (1) as

$$\frac{d\boldsymbol{i}}{dt} = \frac{1}{L}\left(\boldsymbol{e} - \boldsymbol{v} - R\boldsymbol{i}\right). \tag{39}$$

Substituting (37) and (39) into (9) and considering (5), the differentiation of active power can be obtained as

$$\frac{dp}{dt} = \frac{3}{2L}\left[|\boldsymbol{e}|^2 - \mathrm{Re}\left(\boldsymbol{v}^{*}\boldsymbol{e}\right)\right] - \frac{R}{L}p - \omega q^{\mathrm{nov}}. \tag{40}$$

Similarly, the differentiation of reactive power can be obtained from (5), (37), (38), and (39) as

$$\frac{dq^{\mathrm{nov}}}{dt} = \frac{3}{2L}\mathrm{Re}\left[\left(\boldsymbol{e}^{*} - \boldsymbol{v}^{*}\right)\boldsymbol{e}^{'}\right] - \frac{R}{L}q^{\mathrm{nov}} + \omega p. \tag{41}$$

Following the principle of deadbeat power control in conventional DPC-SVM [14], the equations in (40) and (41) can be discretized using first-order Euler method as

$$\begin{aligned}\frac{1}{T_s}\begin{bmatrix} p^{\mathrm{ref}} - p^{k} \\ q^{\mathrm{ref}} - q^{\mathrm{nov},k}\end{bmatrix} &= \frac{3}{2L}\begin{bmatrix} e_\alpha^k e_\alpha^k + e_\beta^k e_\beta^k \\ e_\alpha^k e_\alpha^{'k} + e_\beta^k e_\beta^{'k}\end{bmatrix} \\ &- \begin{bmatrix} \frac{R}{L} & \omega \\ -\omega & \frac{R}{L}\end{bmatrix}\begin{bmatrix} p^k \\ q^{\mathrm{nov},k}\end{bmatrix} - \frac{3}{2L}\begin{bmatrix} e_\alpha^k & e_\beta^k \\ e_\alpha^{'k} & e_\beta^{'k}\end{bmatrix}\begin{bmatrix} v_\alpha^k \\ v_\beta^k\end{bmatrix}.\end{aligned} \tag{42}$$

Solving (42), the final converter voltage reference is calculated as

$$\begin{aligned}\begin{bmatrix} v_\alpha^k \\ v_\beta^k\end{bmatrix} = \begin{bmatrix} e_\alpha^k \\ e_\beta^k\end{bmatrix} &- \frac{2}{3\Delta}\begin{bmatrix} Re_\beta^{'k} + \omega Le_\beta^k & -Re_\beta^k + \omega Le_\beta^{'k} \\ Re_\alpha^{'k} + \omega Le_\alpha^k & -Re_\alpha^k + \omega Le_\alpha^{'k}\end{bmatrix} \\ &\times \begin{bmatrix} p^k \\ q^{\mathrm{nov},k}\end{bmatrix} - \frac{2L}{3T_s\Delta}\begin{bmatrix} e_\beta^{'k} & -e_\beta^k \\ -e_\alpha^{'k} & e_\alpha^k\end{bmatrix}\begin{bmatrix} p^{\mathrm{ref}} - p^k \\ q^{\mathrm{ref}} - q^{\mathrm{nov},k}\end{bmatrix}\end{aligned} \tag{43}$$

where $\Delta = \boldsymbol{e}^k \otimes \boldsymbol{e}^{'k} = e_\alpha^k e_\beta^{'k} - e_\beta^k e_\alpha^{'k}$. It can be seen that the derived converter voltage vector reference in (43) is slightly more complex than the equation in (22) for conventional DPC-SVM, which is mainly caused by the use of extended pq theory [18], [22], [23]. However, compared to other kinds of power control methods under unbalanced grid voltages requiring sequence extraction and complicated power compensation [19], [20], the equation in (43) is considerably simple and easy to implement.

It should be noted that, with the extended pq theory, it is possible to improve the performance of conventional table-based DPC under unbalanced grid voltage conditions. The main problem is how to establish the appropriate switching table, because the extended pq theory itself cannot cope with unbalanced grid voltages automatically. However, the existing switching tables are mostly developed, based on the original pq theory and more efforts have to be done to make them suitable for the extended pq theory. More details regarding the table-based DPC under unbalanced grid voltage conditions would be reported in another paper, so it is not further expanded here.

C. Control Delay Compensation

It is well known that there is a one-step delay in digital implementations, which means that the voltage vector decided at the kth instant will not be applied until the $(k+1)$th instant [28], [29]. However, in prior study for DPC-SVM [5], [14], the one-step delay is not considered. To mitigate the influence of one-step delay, the value at the $(k+1)$th instant should be used in the kth instant. This means that the value at kth instant in the right side of (22) and (43) should be replaced by the value at $(k+1)$ th instant.

The grid current vector at the (k+1)th instant is predicted from (1) as

$$\boldsymbol{i}^{k+1} = \boldsymbol{i}^{k} + \frac{1}{L}\left(\boldsymbol{e}^{k} - R\boldsymbol{i}^{k} - \boldsymbol{v}^{k}\right). \tag{44}$$

Under the assumption of a balanced three-phase system, namely $\boldsymbol{e} = |\boldsymbol{e}|\, e^{j\omega t}$, the grid voltage vector at the $(k+1)$th instant is predicted as

$$\boldsymbol{e}^{k+1} = e^{j\omega T_s}\boldsymbol{e}^{k} \approx \left(1 + j\omega T_s\right)\boldsymbol{e}^{k}. \tag{45}$$

Accordingly, the complex power at the next instant $\boldsymbol{s}^{k+1}$ can be obtained from $\boldsymbol{i}^{k+1}$ and $\boldsymbol{e}^{k+1}$ as

$$\boldsymbol{s}^{k+1} = \frac{3}{2}\left(\boldsymbol{i}^{k+1*}\boldsymbol{e}^{k+1}\right). \tag{46}$$

For the proposed DPC-SVM, the reactive power at the next control period is predicted as

$$\begin{aligned}q^{\mathrm{nov},k+1} = q^{\mathrm{nov},k} + \Bigg(&\frac{3}{2L}\left(\boldsymbol{e}^{k} - \boldsymbol{v}^{k}\right)^{*} \odot \boldsymbol{e}^{'k} \\ &- \frac{R}{L}q^{\mathrm{nov},k} + \omega p^{k}\Bigg)T_s.\end{aligned} \tag{47}$$

After obtaining the prediction for active power and reactive power, they are subsequently applied in (22) and (43) to obtain the desired converter voltage reference for conventional DPC-SVM and the proposed DPC-SVM.

V. Simulation and Experimental Results

A. Simulation Results

To verify the performance of the proposed DPC-SVM under unbalanced conditions, both digital simulations and experimental tests were performed using a two-level three-phase PWM rectifier. The results obtained from conventional DPC-SVM under unbalanced conditions are also presented for comparison. The system and control parameters are listed in Table I, which were used in the simulations and experimental tests. The sampling frequencies of the conventional DPC-SVM and the proposed DPC-SVM are both 10 kHz. Figs. 2 and 3 show the control diagrams for the conventional DPC-SVM and the proposed DPC-SVM, respectively. It can be seen that the differences between

TABLE I
SYSTEM PARAMETERS

System Parameters	Symbol	Value
Line resistance	R	0.3 Ω
Line inductance	L	10 mH
Line-line voltage (RMS)	U_N	150 V
Line voltage frequency	f	50 Hz
Load resistance	R_L	97 Ω
DC-side capacitor	C	840 μF
DC-side voltage	$U_{\rm dc}$	300 V
Sampling period	T_s	100 μs

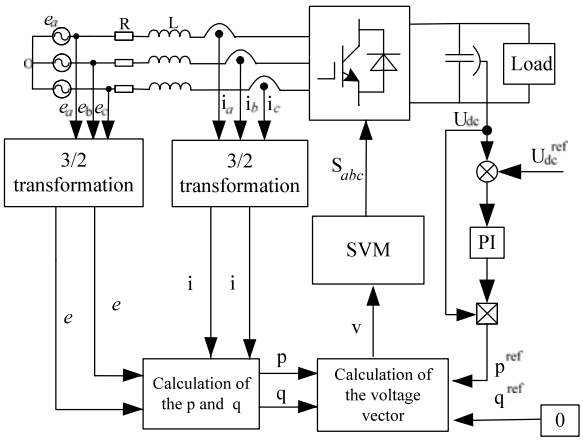

Fig. 2. Control diagram of the conventional DPC-SVM for a PWM rectifier.

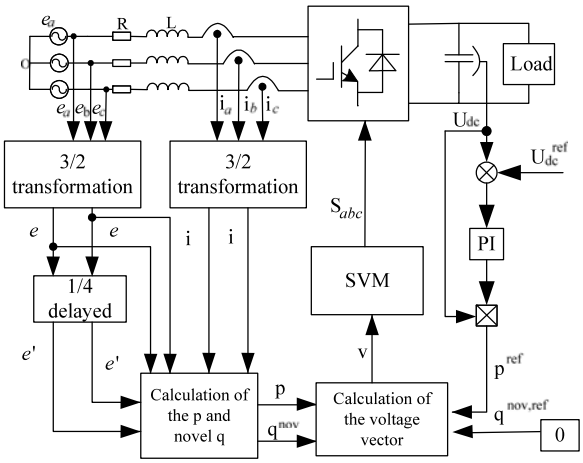

Fig. 3. Control diagram of the proposed DPC-SVM for a PWM rectifier under unbalanced conditions.

the proposed DPC-SVM and conventional DPC-SVM are that the proposed DPC-SVM uses the reactive power in the extended pq theory [18], [22] to calculate the desired converter voltage reference. The rest parts are the same for both DPC-SVM methods. Hence, the conventional DPC-SVM can be easily upgraded to the proposed DPC-SVM. To be clear, the instantaneous reactive power in the original pq theory is called "imaginary power" to distinguish it from the reactive power in the extended pq theory.

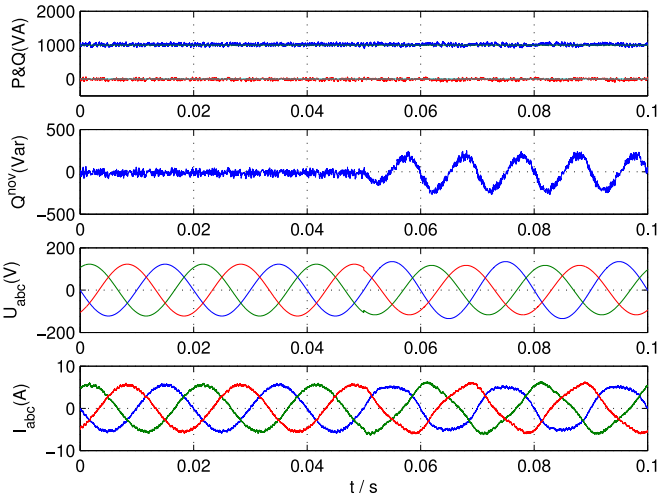

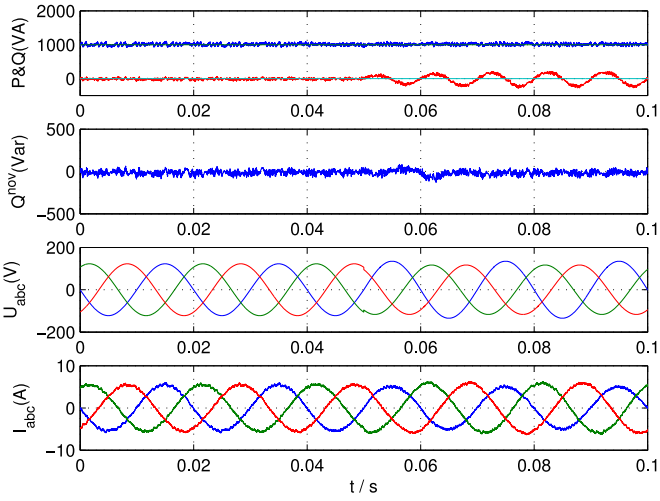

Fig. 4. Simulation results when balanced grid voltages become unbalanced. (a) Conventional DPC-SVM. (b) Proposed DPC-SVM.

Fig. 4 shows the simulations results for both the conventional DPC-SVM and the proposed DPC-SVM when the balanced grid voltages become unbalanced at t =0.05 s. The amplitude of the negative sequence voltage is 10% of that of the positive sequence voltage, namely $|e^-| = 0.1\,|e^+|$. From top to bottom, the curves shown in Fig. 4 are active power, imaginary power, reactive power, three-phase grid voltages, and three-phase grid currents. It is clearly seen that under balanced grid voltages, both methods can achieve sinusoidal grid current, validating that the proposed DPC-SVM does not affect the performance under ideal grid voltages. When the grid voltages become unbalanced, although both active power and imaginary power still tracks their respective reference well, the grid currents are highly distorted and oscillations appear in the reactive power. On the contrary, the grid currents are still sinusoidal in the proposed DPC-SVM, although they are now unbalanced. The imaginary power is now oscillating at twice grid frequency, while the reactive power is constant irrespective of the grid voltage unbalance. The results

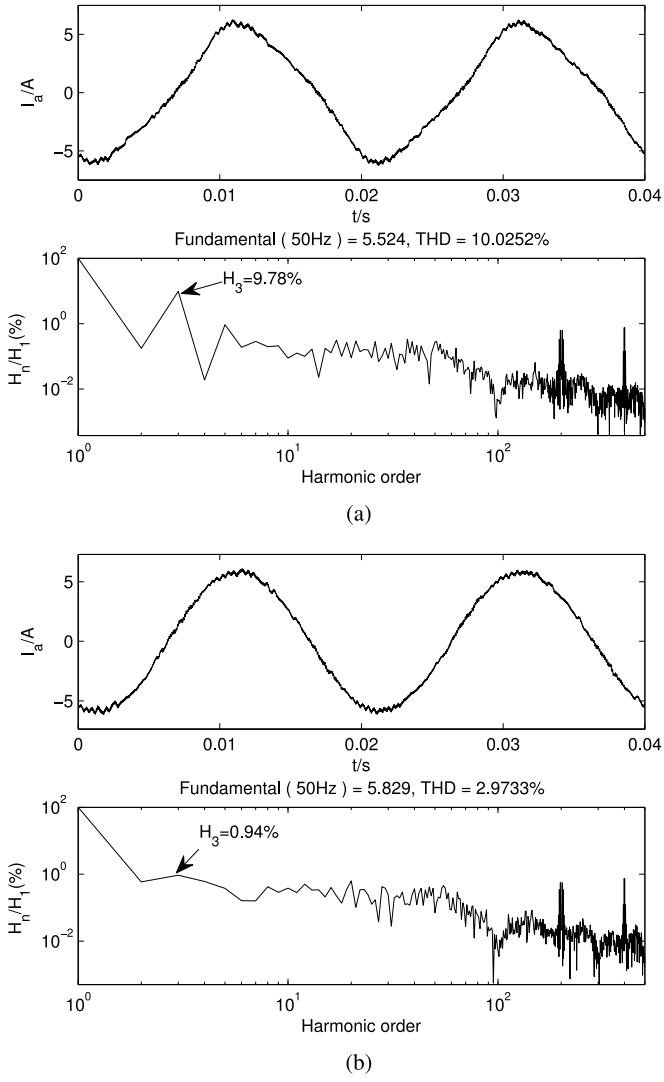

Fig. 5. Simulated harmonic spectra of the grid current at 1000-W active power and 0-Var reactive power for (a) the conventional DPC-SVM, and (b) the proposed DPC-SVM.

prove that the proposed DPC-SVM using the extended pq theory can work well under both balanced and unbalanced grid condition.

Fig. 5 further presents the harmonic spectra of the grid current for the conventional DPC-SVM and the proposed DPC-SVM under unbalanced conditions. It is seen that the grid current is highly distorted and the current THD is up to 10.03% in the conventional DPC-SVM. The triangular shape in the grid current is mainly caused by the third harmonic, which is as high as 9.78%. For the proposed DPC-SVM, the current harmonics (epically the third harmonic) are significantly reduced, and the current THD is only 2.97% under unbalanced grid voltages.

B. Experimental Results

The conventional DPC-SVM and the proposed DPC-SVM were tested under both balanced and unbalanced grid voltage conditions. A 32-bit floating DSP TMS320F28335 was used to accomplish the control algorithms. In the following tests, all variables are displayed on oscilloscope via on-board DA converter except the grid current, which is measured directly by a current probe. The system and control parameters are the same as those listed in Table I. Fig. 6 shows the photograph of the experimental test setup, where the grid voltage unbalance is generated by adding a 5-Ω resistor between the grid and the inductance in phase A to emulate one-phase voltage dip.

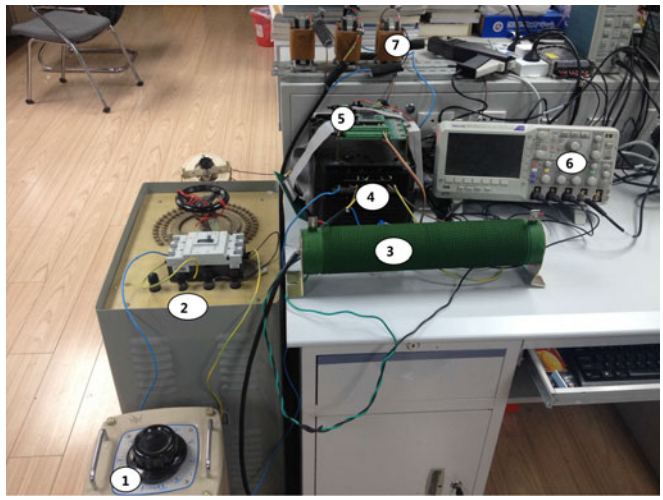

Fig. 6. Experimental test setup. (1) Isolated transformer. (2) 5-Ω resistor in series with phase A. (3) Load resistance. (4) PWM rectifier. (5) DSP control board. (6) Oscilloscope. (7) Line inductance.

The results obtained from the conventional DPC-SVM and the proposed DPC-SVM under the condition of one-phase grid voltage dip are shown in Fig. 7. The active power reference is 1000 W, and the reactive power reference is 0 Var to achieve unity power factor. From top to bottom, the curves shown in Fig. 7 are active power, imaginary power, phase-A grid voltage, and phase-A grid current. It is evident that both methods obtained good performance under ideal grid conditions. However, when the grid voltage dip occurs, the grid current become distorted severely in the conventional DPC-SVM, although both active power and imaginary power are constant. On the contrary, in the proposed DPC-SVM the grid current is still sinusoidal in shape and its amplitude is increased to balance the grid voltage dip. The imaginary power is now oscillating at twice grid frequency. The experimental results are in accordance to the simulation results in Fig. 4, validating the effectiveness of the proposed DPC-SVM under unbalanced grid voltage conditions.

Fig. 8 shows the experimental results when changing from conventional DPC-SVM to the proposed DPC-SVM under unbalanced grid conditions. When the proposed DPC-SVM is enabled, the highly distorted current becomes sinusoidal and the imaginary power begins to oscillate at twice grid frequency. The results confirm the good performance of the proposed DPC-SVM in reducing current harmonics under unbalanced grid voltage conditions.

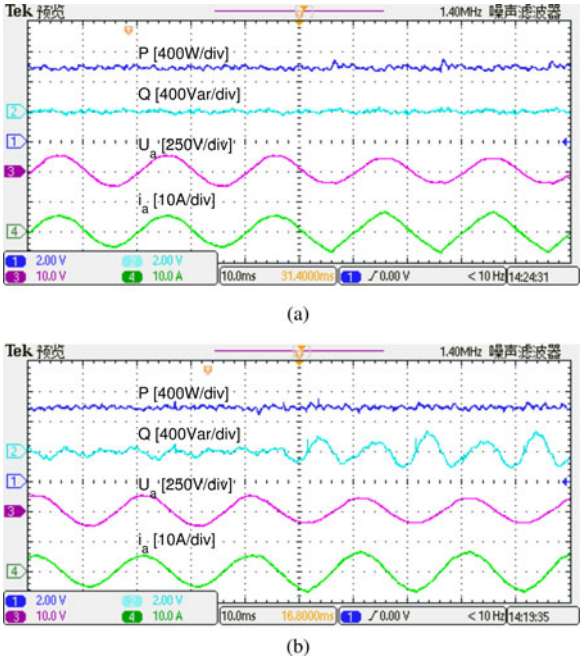

Fig. 7. Responses of active power, imaginary power, one-phase grid voltage, and current under the condition of one-phase grid voltage dip for (a) conventional DPC-SVM, and (b) the proposed DPC-SVM.

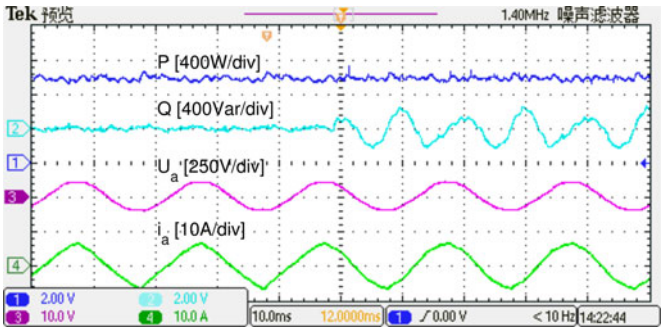

Fig. 8. Responses of active power, imaginary power, one-phase grid voltage, and current when changing from conventional DPC-SVM to the proposed DPC-SVM under unbalanced grid conditions.

As there are only limited channels in the oscilloscope to observer the internal variables, the same tests as Figs. 7 and 8 were performed again in Figs. 9 and 10, where the second curve is now replaced by the reactive power in the extended pq theory. For the conventional DPC-SVM, the reactive power begins to oscillate when the voltage dip occurs. On the contrary, the active power and the reactive power remain constant in the proposed DPC-SVM irrespective of the voltage dip, which differs from the oscillating imaginary power shown in Fig. 7.

Fig. 10 shows that the distorted current become sinusoidal and the oscillation in the reactive power disappears when changing from conventional DPC-SVM to the proposed DPC-SVM. The results are in accordance to the simulation results in Fig. 4. This means that the reactive power, rather than imaginary power, is more suitable for use as the control variable under unbalanced grid voltage conditions.

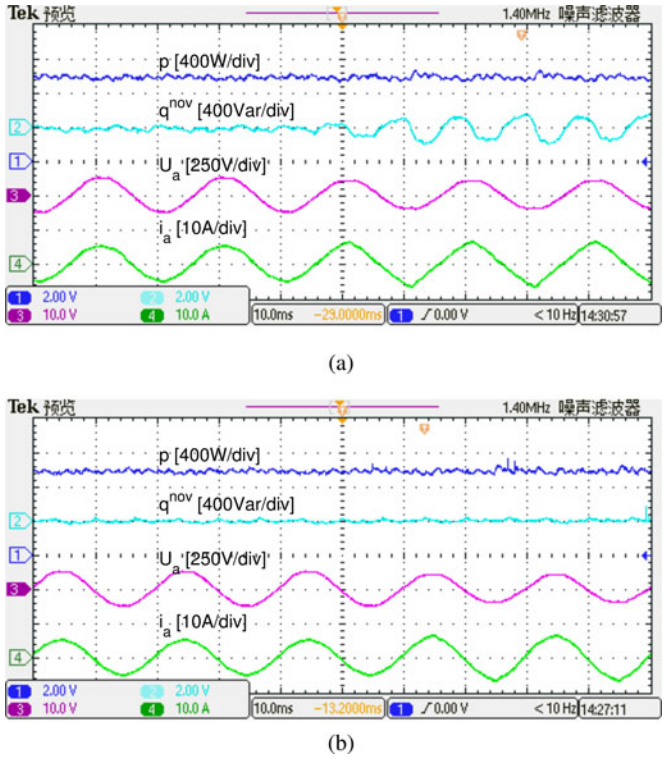

Fig. 9. Responses of active power, reactive power, one-phase grid voltage, and current under the condition of one phase grid voltage dip for (a) conventional DPC-SVM, and (b) the proposed DPC-SVM.

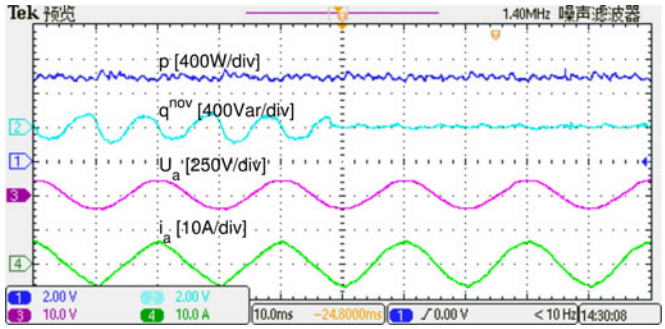

Fig. 10. Responses of active power, reactive power, one-phase grid voltage, and current when changing from conventional DPC-SVM to the proposed DPC-SVM under unbalanced grid conditions.

The experimental test results for the harmonic spectra of the grid current is shown in Fig. 11 for the conventional DPC-SVM and the proposed DPC-SVM under unbalanced grid voltage conditions. Similar to the simulation results in Fig. 5, the grid current in the conventional DPC-SVM is severely distorted and the current THD is as high as 11.08%, which is mainly caused by the third harmonics (8.68%). Much better performance in terms of less harmonics and lower current THD can be obtained in the proposed DPC-SVM. The current THD is only 4.24% and the third harmonic is 1.01%, much lower than the value of conventional DPC-SVM. This confirms the effectiveness of the proposed DPC-SVM in obtaining good quality of grid current.

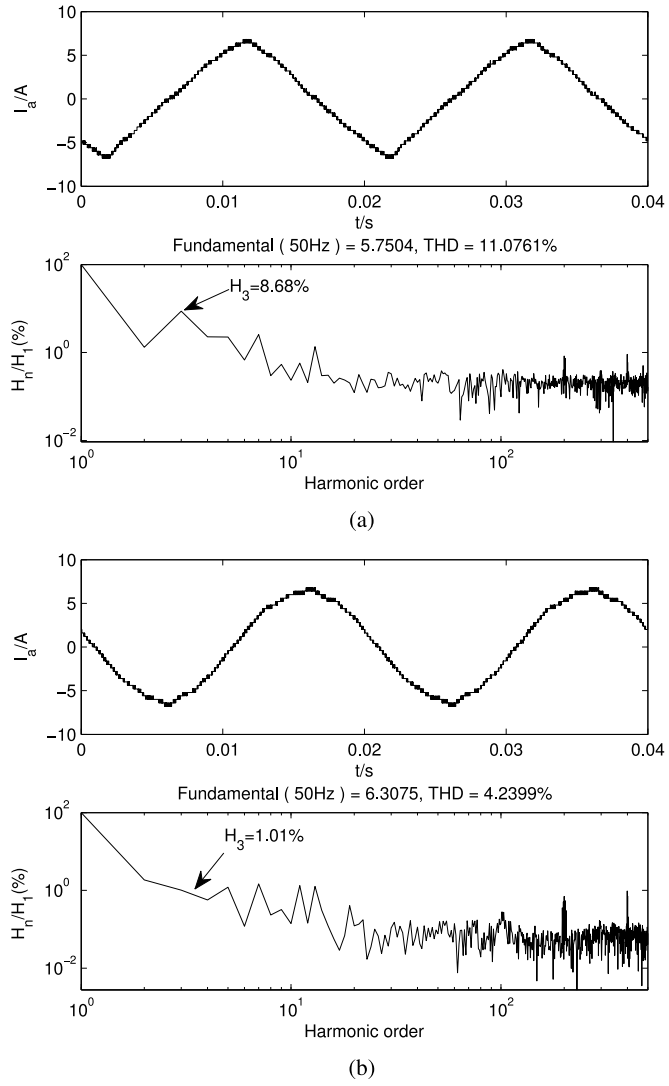

Fig. 11. Harmonic spectra of the grid current when $P = 1000$ W and $Q^{\rm nov} = 0$ Var for (a) conventional DPC-SVM, and (b) the proposed DPC-SVM.

VI. Conclusion

This paper proposes a simple but very effective method to solve the performance deterioration of the conventional DPC-SVM under unbalanced grid voltage conditions. Compared to the conventional DPC-SVM, the control structure remains unchanged except the original pq theory is replaced by an extended pq theory. To adapt the extended pq theory in the proposed method, after deducing the slopes of active power and reactive power, the final converter voltage reference is analytically derived based on the principle of deadbeat control of both active power and reactive power.

Compared to prior DPC based solutions using original pq theory and SVM-based methods using current control and extended pq theory, the proposed DPC-SVM has some obvious advantages. First, no tuning work is required when calculating the converter voltage references, which is easy to use and simple to implement. Second, the control structure is almost the same as conventional DPC-SVM; hence, the conventional DPC-SVM is easy to upgrade to the proposed DPC-SVM without increasing the control complexity too much. Thus, the features of conventional DPC-SVM are fully maintained. Finally, all calculations are implemented in stationary frame without the extraction of positive/negative sequences for the grid voltage/current or complicated power compensation techniques.

The proposed method works effectively under both ideal and unbalanced grid voltage conditions by exhibiting sinusoidal grid current and eliminating the ripples in both active power and the reactive power. A comparative study of the conventional DPC-SVM using original pq theory, and the proposed DPC-SVM is carried out on a two-level three-phase PWM rectifier. The simulations and experimental results confirm the effectiveness of the proposed method.

References

[1] B. Singh, B. N. Singh, A. Chandra, K. Al-Haddad, A. Pandey, and D. P. Kothari, "A review of three-phase improved power quality ac-dc converters," *IEEE Trans. Ind. Electron.*, vol. 51, no. 3, pp. 641–660, Jun. 2004.

[2] J. Rodriguez, J. Dixon, J. Espinoza, J. Pontt, and P. Lezana, "PWM regenerative rectifiers: State of the art," *IEEE Trans. Ind. Electron.*, vol. 52, no. 1, pp. 5–22, Feb. 2005.

[3] V. Blasko and V. Kaura, "A new mathematical model and control of a three-phase ac-dc voltage source converter," *IEEE Trans. Power Electron.*, vol. 12, no. 1, pp. 116–123, Jan. 1997.

[4] T. Noguchi, H. Tomiki, S. Kondo, and I. Takahashi, "Direct power control of PWM converter without power-source voltage sensors," *IEEE Trans. Ind. Appl.*, vol. 34, no. 3, pp. 473–479, May/Jun. 1998.

[5] M. Malinowski, M. Jasinski, and M. Kazmierkowski, "Simple direct power control of three-phase PWM rectifier using space-vector modulation (DPC-SVM)," *IEEE Trans. Ind. Electron.*, vol. 51, no. 2, pp. 447–454, April 2004.

[6] Y. Zhang, Z. Li, Y. Zhang, W. Xie, Z. Piao, and C. Hu, "Performance improvement of direct power control of PWM rectifier with simple calculation," *IEEE Trans. Power Electron.*, vol. 28, no. 7, pp. 3428–3437, Jul. 2013.

[7] Y. Zhang, J. Long, Y. Zhang, T. Lu, Z. Zhao, and L. Jin, "Table-based direct power control for three-level neutral point-clamped pulse-width modulated rectifier," *IET Power Electron.*, vol. 6, no. 8, pp. 1555–1562, 2013.

[8] Y. Zhang, W. Xie, and Y. Zhang, "Deadbeat direct power control of three-phase pulse-width modulation rectifiers," *IET Power Electron.*, vol. 7, no. 6, pp. 1340–1346, 2014.

[9] J. Alonso-Martinez, J. E. Carrasco, and S. Arnaltes, "Table-based direct power control: A critical review for microgrid applications," *IEEE Trans. Power Electron.*, vol. 25, no. 12, pp. 2949–2961, Dec. 2010.

[10] Y. Zhang and W. Xie, "Low complexity model predictive control—single vector-based approach," *IEEE Trans. Power Electron.*, vol. 29, no. 10, pp. 5532–5541, Oct. 2014.

[11] Y. Zhang, W. Xie, Z. Li, and Y. Zhang, "Low-complexity model predictive power control: Double-vector-based approach," *IEEE Trans. Ind. Electron.*, vol. 61, no. 11, pp. 5871–5880, Nov. 2014.

[12] P. Cortes, J. Rodriguez, P. Antoniewicz, and M. Kazmierkowski, "Direct power control of an AFE using predictive control," *IEEE Trans. Power Electron.*, vol. 23, no. 5, pp. 2516–2523, Sep. 2008.

[13] Y. Zhang, W. Xie, Z. Li, and Y. Zhang, "Model predictive direct power control of a PWM rectifier with duty cycle optimization," *IEEE Trans. Power Electron.*, vol. 28, no. 11, pp. 5343–5351, Nov. 2013.

[14] A. Bouafia, J.-P. Gaubert, and F. Krim, "Predictive direct power control of three-phase pulsewidth modulation (PWM) rectifier using space-vector modulation (SVM)," *IEEE Trans. Power Electron.*, vol. 25, no. 1, pp. 228–236, Jan. 2010.

[15] J. Fischer, S. Gonzalez, I. Carugati, M. Herran, M. Judewicz, and D. Carrica, "Robust predictive control of grid-tied converters based on direct power control," *IEEE Trans. Power Electron.*, vol. 29, no. 10, pp. 5634–5643, Oct. 2014.

[16] D. Koval, "Power system disturbance patterns," *IEEE Trans. Ind. Appl.*, vol. 26, no. 3, pp. 556–562, May/Jun. 1990.

[17] A. Stankovic and T. Lipo, "A novel control method for input output harmonic elimination of the PWM boost type rectifier under unbalanced operating conditions," *IEEE Trans. Power Electron.*, vol. 16, no. 5, pp. 603–611, Sep. 2001.
[18] Y. Suh and T. A. Lipo, "Modeling and analysis of instantaneous active and reactive power for PWM AC/DC converter under generalized unbalanced network," *IEEE Trans. Power Del.*, vol. 21, no. 3, pp. 1530–1540, Jul. 2006.
[19] J. Eloy-Garcia, S. Arnaltes, and J. Rodriguez-Amenedo, "Direct power control of voltage source inverters with unbalanced grid voltages," *IET Power Electron.*, vol. 1, no. 3, pp. 395–407, 2008.
[20] L. Shang, D. Sun, and J. Hu, "Sliding-mode-based direct power control of grid-connected voltage-sourced inverters under unbalanced network conditions," *IET Power Electron.*, vol. 4, no. 5, pp. 570–579, 2011.
[21] H. Akagi, Y. Kanazawa, and A. Nabae, "Instantaneous reactive power compensators comprising switching devices without energy storage components," *IEEE Trans. Ind. Appl.*, vol. IA-20, no. 3, pp. 625–630, May 1984.
[22] Y. Komatsu and T. Kawabata, "A control method of active power filter where system voltage contains negative-phase-sequence component or zero-phase-sequence component," in *Proc. Int. Power Electron. Drive Syst. Conf.*, 1995, pp. 583–586.
[23] Y. Komatsu and T. Kawabata, "A control method of active power filter in unsymmetrical voltage system," in *Proc. Int Power Electron. Drive Syst.Conf.* 1997, vol. 2, pp. 839–843.
[24] Y. Suh and T. A. Lipo, "Control scheme in hybrid synchronous stationary frame for PWM AC/DC converter under generalized unbalanced operating conditions," *IEEE Trans. Ind. Appl.*, vol. 42, no. 3, pp. 825–835, May/Jun. 2006.
[25] Z. Li, Y. Li, P. Wang, H. Zhu, C. Liu, and W. Xu, "Control of three-phase boost-type PWM rectifier in stationary frame under unbalanced input voltage," *IEEE Trans. Power Electron.*, vol. 25, no. 10, pp. 2521–2530, Oct. 2010.
[26] A. V. Timbus, P. Rodriguez, R. Teodorescu, M. Liserre, and F. Blaabjerg, "Control strategies for distributed power generation systems operating on faulty grid," in *Proc. IEEE Int. Symp. Ind. Electron*, 2006, vol. 2, pp. 1601–1607.
[27] H.-S. Song and K. Nam, "Dual current control scheme for PWM converter under unbalanced input voltage conditions," *IEEE Trans. Ind. Electron.*, vol. 46, no. 5, pp. 953–959, Oct. 1999.
[28] Y. Zhang, J. Zhu, and W. Xu, "Analysis of one step delay in direct torque control of permanent magnet synchronous motor and its remedies," in *Proc. Int. Conf. Electr. Mach. Syst.*, 2010, pp. 792–797.
[29] P. Cortes, J. Rodriguez, C. Silva, and A. Flores, "Delay compensation in model predictive current control of a three-phase inverter," *IEEE Trans. Ind. Electron.*, vol. 59, no. 2, pp. 1323–1325, Feb. 2012.

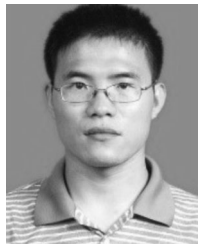

Yongchang Zhang (M' 10) received the B.S. degree from Chongqing University, Chongqing, China, in 2004, and the Ph.D. degree from Tsinghua University, Beijing, China, in 2009, both in electrical engineering.

From August 2009 to August 2011, he was a Postdoctoral Fellow with the University of Technology Sydney, Australia. He joined the North China University of Technology, Beijing, in August 2011, and became an Associate Professor in power electronics and motor drives. He has published more than 70 technical papers in the area of motor drives, pulsewidth modulation and ac/dc converters. His current research interests include model predictive control for power converters and motor drives.

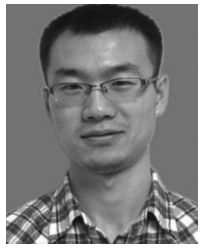

Changqi Qu (S'14) was born in 1988. He received the B.S. degree from Beijing Jiaotong University, Beijing, China, in 2010. He is currently working toward the master's degree in electrical engineering at the North China University of Technology, Beijing, China.

His research interest includes control of PWM rectifiers under unbalanced grid voltages.